2). Furthermore, this phenomenon was insensitive to the details of the initial state (for example, bodies of equal size versus a power-law distribution, initial eccentricities as low as 10^{-3}, or number of initial bodies). Inclusion of tidal disruption after close encounters to an extent considerably greater than that permitted (*11*) also did not affect this conclusion. For these reasons it is believed that if terrestrial planets accumulated from smaller bodies (at least if gas drag can be ignored), this accumulation was accompanied by the impact of very large bodies. In the case of Earth, the mass of these bodies was up to three times that of Mars.

The dominance of these large impacts during the growth of Earth (and Venus) may be expected to have important consequences.

1) The kinetic energy ($\sim 5 \times 10^{38}$ ergs) released in the largest impacts (1.5×10^{27} g at ~9 km/sec) would be several times greater than that required to melt the entire Earth. Collisions of this size would be highly inelastic. Because the mass of the impacting body is comparable to that of the target, this energy would be distributed over a large fraction of the total volume of the resulting combined body. As a result of these largest impacts, in combination with many more smaller but still massive impacts, as Earth grew it would have been at least partially melted throughout. Core formation by gravitational segregation of metallic iron would proceed simultaneously with the growth of Earth and would not represent a separate later event.

2) It is likely that major quantities of both Earth and the largest projectile would vaporize and recondense in geocentric orbit (*13*). This may have been sufficient to form the moon and could account in a natural way for the large angular momentum of the Earth-moon system, a result that would have been difficult to achieve if the accumulation had been dominated by small bodies of near zero average angular momentum (*1, 13*). This may also explain chemical differences and similarities between Earth and the moon (*14*). The absence of a moon of Venus could have resulted from possible tidal evolution histories that gave rise to either escape into heliocentric orbit or impact with Venus (*15*).

3) These giant impacts also would have removed a primordial terrestrial atmosphere, even one considerably larger than our present atmosphere (*16*). This raises the possibility that the difference in the content of inert gases of Earth and Venus could simply reflect differences in the gravitationally captured atmosphere in equilibrium with the greatly depleted solar nebula at the time of the last atmosphere-removing impact. The xenon-formation age of Earth's atmosphere (~10^8 years) may also date this event in some general way (*17*).

GEORGE W. WETHERILL
Department of Terrestrial Magnetism, Carnegie Institution of Washington, Washington, D.C. 20015

References and Notes

1. W. K. Hartmann and D. R. Davis, *Icarus* **24**, 504 (1975).
2. G. W. Wetherill, *Proc. Lunar Sci. Conf.* **7**, 3245 (1976).
3. Y. Nakagawa, C. Hayashi, K. Nakazawa, *Icarus* **54**, 361 (1983). Multiplanet accumulation has not been calculated for a gaseous nebula. Comparison of the work cited above, "particles-in-a-box" gas-free calculations, and the present work suggests that giant impacts will also occur during multiplanet accumulation in a gaseous nebula.
4. G. W. Wetherill, *Annu. Rev. Astron. Astrophys.* **18**, 77 (1980); *Geol. Soc. Canada Spec. Pap. 20* (1980), p. 3.
5. L. P. Cox and J. S. Lewis, *Icarus* **44**, 706 (1980).
6. K. E. Edgeworth, *Mon. Not. R. Astron. Soc.* **109**, 600 (1949); V. S. Safronov, *Vopr. Kosmog.* **7**, 121 (1960); P. Goldreich and W. R. Ward, *Astrophys. J.* **183**, 1051 (1973).
7. R. Greenberg, J. F. Wacker, W. K. Hartmann, C. R. Chapman, *Icarus* **35**, 1 (1978).
8. G. Wetherill and L. P. Cox, *ibid.* **60**, 40 (1984); submitted to *Icarus*.
9. J. W. Dohnanyi, *J. Geophys. Res.* **74**, 2531 (1969).
10. J. R. Arnold, *Astrophys. J.* **141**, 1536 (1965).
11. V. S. Safronov, *Evolution of the Protoplanetary Cloud and Formation of the Earth and Planets* (Nauka, Moscow, 1969) (translation NASA TTF-677, 1972).
12. H. Mizuno and A. P. Boss, *Icarus*, in press.
13. A. G. W. Cameron and W. R. Ward, *Lunar Sci.* **7**, 120 (1976); *Lunar Planet. Sci.* **9**, 1205 (1978); A. C. Thompson and D. J. Stevenson, *ibid.* **14**, 787 (1983).
14. A. E. Ringwood, *Proceedings of the Apollo 11 Lunar Science Conference* (Pergamon, New York, 1970), pp. 769–799.
15. C. C. Counselman, *Astrophys. J.* **180**, 307 (1973).
16. A. G. W. Cameron, *Icarus* **56**, 195 (1983).
17. G. W. Wetherill, *Annu. Rev. Nucl. Sci.* **25**, 283 (1975); R. O. Pepin and D. Phinney, *Lunar Sci.* **7**, 682 (1976).
18. Supported by NASA grant NSG 7397. This work is also part of a larger program at the Department of Terrestrial Magnetism supported by NASA grant NAGW 398. I thank A. P. Boss, H. Mizuno, and D. R. Stevenson for discussions.

21 December 1984; accepted 26 February 1985

Expression of the Major Surface Antigen of *Plasmodium knowlesi* Sporozoites in Yeast

Abstract. *The circumsporozoite protein, a surface antigen of the sporozoite stage of the monkey malarial parasite* Plasmodium knowlesi, *was expressed in the yeast* Saccharomyces cerevisiae *by using an expression vector containing the 5′ regulatory region of the yeast alcohol dehydrogenase I gene. It was necessary to eliminate the entire 5′ upstream region of the parasite DNA to obtain the expression of this protein. Only the circumsporozoite precursor protein was produced by the yeast transformants, as detected by immunoblotting. About 55 and 20 percent of the circumsporozoite protein produced in yeast was associated with the 25,000*g *and 150,000*g *particulate fractions, respectively. The protein could be solubilized in Triton X-100 and was stable in solubilized extracts.*

Radiation-attenuated *Plasmodium* sporozoites confer protective immunity against malaria in a number of animal species (*1*). The major sporozoite surface protein, the circumsporozoite (CS) protein, has been implicated as the protective antigen (*2, 3*). We earlier reported the cloning of the CS gene from the simian malarial parasite *Plasmodium knowlesi* (*4, 5*), and this opened the way to obtain quantities of the CS protein by expression in suitable host systems. The original *Escherichia coli* construction containing the *P. knowlesi* CS gene expressed the surface antigen as the β-lactamase fusion protein (*4*). For structural and vaccination studies, however, it is important to express the CS gene as a complete protein, with little or no difference from the parasite protein. Recently we reported (in collaboration with the NIH group of B. Moss) the construction of a recombinant vaccinia virus that expresses the complete *P. knowlesi* CS protein in infected monkey cell line CV-1 (*6*). The recombinant virus is antigenic in rabbits, and its vaccine potential is under evaluation. However, whether such a recombinant vaccinia virus vaccine would be safe and effective in humans is not known (*7*). Among the possible options, recombinant yeast appears to be a safe source of antigen and has been successfully used to produce a vaccine effective against the hepatitis B virus infection (*8, 9*). Here we describe the expression of the complete CS protein of *P. knowlesi* in the yeast *Saccharomyces cerevisiae*, as obtained with an expression vector containing the 5′ regulatory region of the yeast alcohol dehydrogenase I gene.

The CS protein–encoding sequence used was isolated on an Aha III–Aha III fragment of 1.6 kilobase pairs (kb) present in the λkm15 clone, originally isolated from a *P. knowlesi* merozoite DNA Charon 4A library (*5*). It was necessary to eliminate as much as possible the 5′ upstream region of the CS gene sequence

Table 1. Distribution of the CS protein in different particulate fractions of yeast cells. A detailed description of the experiment is given in the legend to Fig. 2.

Fraction	CS protein (units*)			Total protein (mg)			CS protein (percent)		Relative abundance (unit/mg)	
	ypSG22	ypSG19	ypMA56	ypSG22	ypSG19	ypMA56	ypSG22	ypSG19	ypSG22	ypSG19
Total cell suspension	3.33	4.05	0	3.91	3.75	5.70	100	100	0.85	1.08
25,000*g* pellet	1.64	2.61	0	0.29	0.45	0.50	50	64	5.66	5.80
150,000*g* pellet	1.02	0.56	0	0.46	0.50	0.75	31	14	2.22	1.12
150,000*g* supernatant	0.85	0.85	0	2.99	3.38	3.90	26	21	0.28	0.25

*Arbitrary units calculated from a densitometer tracing of a positive film of the immunoblot using a dual-wavelength chromatographic scanner (Shimadzu model CS910). Each unit represents 10^3 μV/msec absorbed at 510 nm.

because in prior experiments yeast transformants containing the entire Aha III–Aha III fragment, with 260 base pairs (bp) preceding the start of the CS gene coding sequences, failed to express the CS protein. Therefore the Aha III fragment was cleaved with Xmn I, which cut 7 bp 3′ to the ATG initiation codon (A, adenine; T, thymine; G, guanine). The ATG was provided in the correct reading frame by adding synthetic Nde I linkers (CCATATGG) (C, cytosine). By such a construction the amino terminal amino acid sequence was changed to Met-Asp-Phe- instead of the authentic Met-Lys-Asn-Phe-. The yeast ADH I expression vector, pMA56 (*10*), was cleaved with Eco RI endonuclease and treated with nuclease S1 to remove the 3′ overhang. This treatment ensured the placement of an A-residue in the −4 position in the leader region, which has been suggested to provide more efficient translation initiation by yeast ribosomes (*11*). In the clone described, the nuclease S1 treatment removed not only the 3′ overhang but also the first G-residue of the Eco RI linker provided in the vector. This resulted in the placement of A-residues in both the −3 and −4 positions, which is considered even better for translation initiation (*11*). The exact construction of the hybrid plasmid is shown in Fig. 1. The nucleotide sequence at the junction of the yeast ADH I promoter region and the CS gene was confirmed by DNA sequence analysis. Yeast cells (D13-1A) were transformed with the recombinant plasmid by using standard transformation procedures, with *TRP1*$^+$ as the selection marker (*12*).

Cell extracts from 12 Trp$^+$ yeast transformants, grown to mid-log phase, were assayed for the CS protein by immunoenzyme assay with polyclonal serum from rhesus monkeys injected with irradiated sporozoites. A distinct CS protein band could be detected in each of the transformants by using ~2 μg of total protein, corresponding to 15 μl of the cell cultures (~10^5 cells). From the enzyme immunoassay, which detects about 100 pg of antigen, we estimate that at least ~1 μg of CS protein is produced by 150 ml of culture (or 1 μg of CS protein per 20 mg of total protein). Two of the positive cell lines, ypSG19 and ypSG22, were selected for further characterization. These cells grew more slowly (doubling time, 5 hours) than the control cells (line ypMA56) containing the vector pMA56 alone (doubling time, 3 hours). The level of CS protein detected in these cultures was substantial, while the control cells showed no corresponding CS protein band (Fig. 2).

We cloned the CS gene almost exactly from its own ATG initiation codon. In the hybrid plasmid pSG22, the CS gene is flanked on the 5′ side by the yeast alcohol dehydrogenase promoter region and on the 3′ end by the replication origin of yeast from the 2-μm circle. One can, therefore, assume that the parasite translation termination signal present in the cloned sequence is recognized by yeast translation machinery. Therefore the CS protein made in yeast must be derived from the nearly complete coding region residing between the Xmn I site and 1090 bp of the CS gene. This is supported by the observation that the yeast CS protein is the same size as the wheat germ translation product of the sporozoite messenger RNA in vitro, both of these being about 1000 daltons smaller than the authentic parasite CS

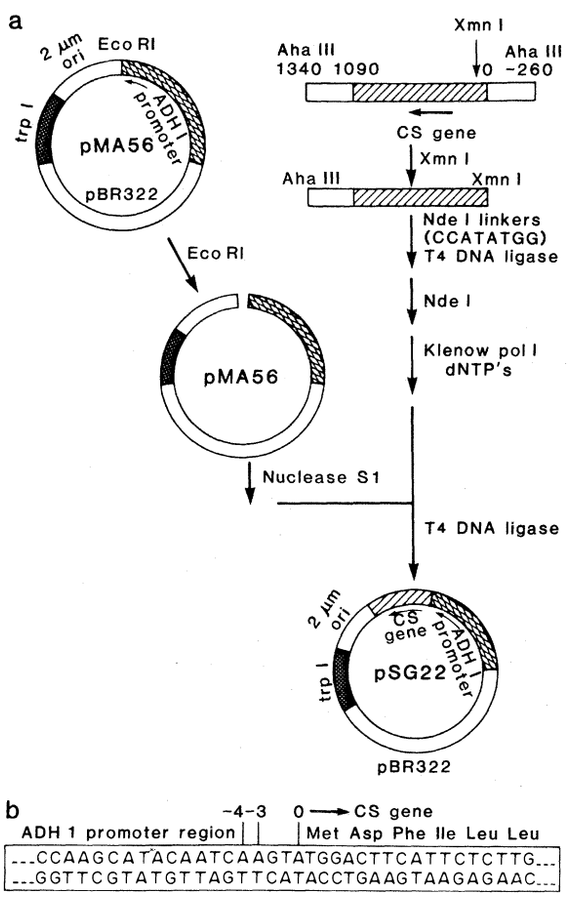

Fig. 1. (a) Construction of the hybrid plasmid containing the yeast ADH1 promoter region directly fused to the CS gene of *Plasmodium knowlesi*. Two micrograms of the 1.6-kb Aha III fragment containing the entire CS gene, obtained from the original genomic clone (*5*) by electroelution, was digested with Xmn I. Nde I linkers (New England Biolabs) were kinased with [γ^{32}P]adenosine triphosphate and the kinased linkers were ligated to the Xmn I–Aha III fragment (12 hours at 4°C). The DNA was then digested with Nde I and the linker ligated fragment was isolated by electroelution and ligated to 0.4 μg of the vector pMA56 (previously digested with Eco RI and treated with nuclease S1). *Escherichia coli* HB101 cells were transformed and the clone containing the fragment in the correct orientation was identified by plasmid minipreps. Plasmid preparations were made and yeast cells D13-1A (a *trp*1-289 *his*3-532 *gal*2) (*26*) were transformed (*12*). Transformants were selected on yeast synthetic medium lacking tryptophan. (b) DNA sequence of the ADH I–CS protein gene junction present in pSG22. The sequence was determined by the Sanger dideoxy chain termination method (*24*) after subcloning the relevant junction fragment into sequencing vector M13mp8 (*25*).

protein precursor in vivo (*4*). The small size difference could be due to a post-transcriptional or posttranslational modification. However, the yeast CS protein appears to be much more similar to the authentic CS protein, as compared to the CS protein produced in cells infected with the recombinant vaccinia virus (*6*). In the latter, two major polypeptides are produced that are heavier than the precursor CS protein by 3000 to 4000 daltons. The yeast CS protein is also remarkably stable, unlike the comparable protein expressed in prokaryotic systems, which exhibits a distinct ladder of degradation products. Such ladders have also been reported for other surface antigens of *Plasmodium* cloned into bacterial systems (*13*).

The sizes of the sporozoite CS protein precursors have been reported to be 52 and 50 kD on sodium dodecyl sulfate (SDS) gels, and that of the processed CS protein as 42 kD. The bands of 52 and 50 kD often do not resolve in SDS gels (*6*). Under our conditions of SDS–polyacrylamide gel electrophoresis, we observed the sporozoite CS protein bands at 66 and 51 kD and the yeast CS protein band at 64.5 kD (Figs. 2 and 3). The differences in sizes could be attributed to abnormal SDS binding of the antigen. Several membrane proteins exhibit anomalous behavior on SDS gels (*14, 15*). The affinity-purified CS protein of *P. berghei* varied in apparent size between 46 to 57 kD depending on the SDS gel running conditions (*16*).

In the initial screening for positive transformants Triton X-100 was included in the extraction buffer. To test the subcellular distribution of this protein, we ruptured the cells in an osmotic medium (0.5*M* sorbitol) with glass beads and subjected them to differential centrifugation. The distribution of the protein in different particulate fractions is shown in Fig. 2 and Table 1. About 50 to 60 percent of the protein was associated with the 25,000*g* pellet, which normally brings down all subcellular organelles, and another 15 to 30 percent of it was associated with 150,000*g* pellet. The latter accounts for small particulate membrane fractions, while the 150,000*g* supernatant represents the cytosolic fraction (*17*). Thus the particulate fractions account for greater than 75 percent of the CS protein in yeast. In terms of specific activity, the 25,000*g* fraction was found to be about 20 times and the 150,000*g* fraction five to ten times richer than the cytosolic fraction (Table 1).

To ascertain whether self-aggregation causes the yeast CS protein to pellet at 25,000*g*, we studied the sedimentation velocity distribution of the protein on a sucrose density gradient (Fig. 3). The CS protein peak sedimented between bovine serum albumin (BSA; molecular weight 67,000) and ovalbumin (molecular weight, 43,000) with a sedimentation coefficient of 3.5*S* (*18*). The CS protein migrated as a monomer and did not aggregate. This is in contrast to the hepatitis B surface antigen expressed in yeast, which aggregates under similar conditions to form the Dane particle, which is comparable to the authentic hepatitis B surface antigen (sedimentation coefficient, 55*S*) (*8*). There are no data on the sedimentation behavior of the sporozoite CS protein under nondenaturing conditions, hence we are unable to compare the yeast CS protein with that of sporozoite. Under denaturing conditions in SDS-urea, the sporozoite CS protein sediments between BSA and ovalbumin (*19*).

No CS protein could be detected in the yeast culture medium. This was expected since the CS protein is a surface antigen and not a secretory protein.

In conclusion, the CS protein produced in yeast was very similar to the authentic sporozoite CS protein precursor. It was largely associated with the 25,000*g* and 150,000*g* particulate frac-

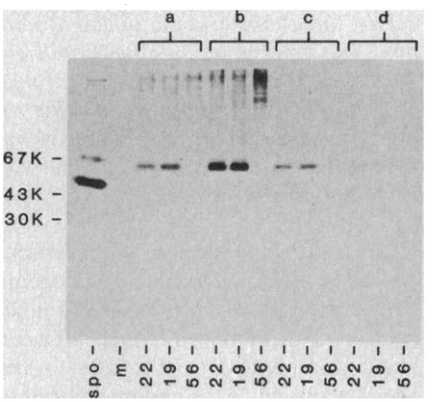

Fig. 2. Immunoenzyme blot of yeast transformants after differential centrifugation. Lanes 22, 19, and 56 represent cell lines ypSG22, ypSG19, and the control ypMA56, respectively; spo, sporozoites; m, molecular weight markers; a, total cell extract; b, 25,000*g* pellet suspension; c, 150,000*g* pellet suspension; and d, 150,000*g* supernatant. In lanes a and d 7 μg of protein and in lanes b and c 3.5 μg of protein were placed on the SDS gel. Cells, grown in 50 ml of yeast synthetic complete medium lacking tryptophan, were pelleted, washed in 10 ml of sorbitol buffer [0.5*M* sorbitol, 10 m*M* phosphate buffer (*p*H 7.5), and 1 m*M* phenylmethylsulfonyl fluoride (PMSF)], suspended in 4 ml of the same buffer, and vortexed with 5 g of glass beads for 2 minutes at 4°C. After centrifugation at 3000*g* to remove intact cells, cell debris, and glass beads, the homogenate was centrifuged at 25,000*g* for 20 minutes. The supernatant was then centrifuged at 150,000*g* for 60 minutes. The pellets were drained completely and resuspended in 10 m*M* phosphate buffer (*p*H 7.5) containing 0.1 percent Triton X-100 and 1 m*M* PMSF by means of a small Teflon homogenizer. The total protein present in each fraction was estimated by Bio-Rad protein assay with BSA as the standard. Each fraction was solubilized in SDS and resolved by electrophoresis on 10 percent SDS–polyacrylamide gel. SDS-solubilized extracts of sporozoites were run on the same gel. Proteins were transblotted onto nitrocellulose (Bio-Rad Transblot cell). An immunoenzyme assay was carried out with polyclonal rhesus monkey serum raised against irradiated sporozoites as the first antibody and horseradish peroxidase–conjugated goat antibody to monkey serum (Cappel) as the second.

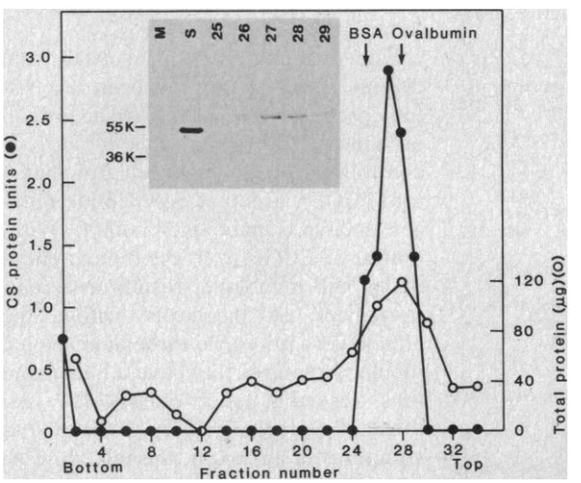

Fig. 3. Sucrose gradient sedimentation pattern of the CS protein from yeast. A 200-ml culture of ypSG22 was grown in tryptophan-free medium, harvested at mid-log phase, and vortexed with glass beads and extraction buffer [10 m*M* phosphate buffer (*p*H 7.5), 0.1 percent Triton X-100, and 1 m*M* PMSF]. After centrifugation at 3000*g*, the supernatant was treated with $(NH_4)_2SO_4$ to 50 percent saturation. The precipitate was resuspended in extraction buffer and dialyzed overnight against the same buffer. A 0.5-ml portion (total protein, ~2 mg), together with 10 μg each of BSA and ovalbumin, was layered on a 5 to 20 percent sucrose gradient in 10 m*M* phosphate buffer (*p*H 7.5) containing 150 m*M* NaCl and run at 38,000 rev/min at 4°C for 18 hours in a Beckman SW 41 rotor. Fractions (0.35 ml) were collected and each fraction was resolved on a 10 percent SDS gel, transblotted, and assayed for CS protein as described in the legend to Fig. 2. The inset shows the immunoblot of the peak fractions. Lane M, molecular weight markers; S, SDS-solubilized sporozoites. CS protein units are defined in Table 1.

tions, could be solubilized by Triton X-100, and was stable in the solubilized extracts.

The CS protein gene is representative of the *Plasmodium* surface antigens that have been cloned and characterized so far. These include the CS protein of *P. knowlesi* (*5*) and *P. falciparum* (*20, 21*), the S-antigen (*13*), the ring-infected erythrocyte surface antigen (*22*), and the pPF11-1 antigen (*23*) of *P. falciparum*. Each of these surface antigens contains many copies of a highly conserved, tandemly repeated peptide unit made of 4 to 12 amino acids. In the case of the CS proteins, where the complete genes have been isolated and sequenced, the repeated peptide units constitute ~40 percent of the polypeptide chain (*5, 20*). These units were found to be the most immunogenic parts of these proteins, as almost all monoclonal antibodies isolated against the sporozoite were directed against the repeated epitope (*2*). As has been pointed out (*22*), the repeats may mask an immune response directed against other surface antigens or against a different hapten on the same molecule. With the purification of the CS protein it will be possible to study the second hypothesis, namely whether peptide sequences other than the repeated units would make a more effective protective antibody than the repeated polypeptide or the entire protein.

SHOBHONA SHARMA
G. NIGEL GODSON
Department of Biochemistry, New York University Medical Center, New York 10016

References and Notes

1. R. Nussenzweig, *Int. J. Nucl. Med. Biol.* **7**, 89 (1980).
2. A. Cochrane, F. Santoro, V. Nussenzweig, R. Gwadz, R. S. Nussenzweig, *Proc. Natl. Acad. Sci. U.S.A.* **79**, 5651 (1982).
3. E. H. Nardin *et al.*, *J. Exp. Med.* **156**, 20 (1982).
4. J. Ellis *et al.*, *Nature (London)* **302**, 536 (1983).
5. L. S. Ozaki, P. Svec, R. S. Nussenzweig, V. Nussenzweig, G. N. Godson, *Cell* **34**, 815 (1983).
6. G. L. Smith *et al.*, *Science* **224**, 397 (1984).
7. J. Beale, *Nature (London)* **311**, 12 (1984).
8. P. Valenzuela, A. Medina, W. J. Rutter, G. Ammerer, B. D. Hall, *ibid.* **298**, 347 (1982).
9. W. J. McAleer *et al.*, *ibid.* **307**, 178 (1984).
10. G. Ammerer, *Methods Enzymol.* **101**, 192 (1983).
11. R. A. Hitzeman *et al.*, *Nature (London)* **293**, 717 (1981).
12. F. Sherman, G. R. Fink, J. B. Hicks, *Methods in Yeast Genetics* (Cold Spring Harbor Laboratory, Cold Spring Harbor, N.Y., 1981).
13. R. L. Coppel *et al.*, *Nature (London)* **306**, 751 (1983).
14. R. N. Frank and D. Rodbard, *Arch. Biochem. Biophys.* **171**, 1 (1975).
15. C. Tanford and J. A. Reynolds, *Biochim. Biophys. Acta* **457**, 133 (1976).
16. A. Vermeulen, thesis, Katholieke Universiteit Nijmegen, Nijmegen, Netherlands (1983).
17. P. Matile, M. Cortat, A. Wiemken, A. Frey-Wyssling, *Proc. Natl. Acad. Sci. U.S.A.* **68**, 636 (1971).
18. R. G. Martin and B. N. Ames, *J. Biol. Chem.* **236**, 1372 (1961).
19. F. Zavala, A. H. Cochrane, E. H. Nardin, R. S. Nussenzweig, V. Nussenzweig, *J. Exp. Med.* **157**, 1947 (1983).
20. J. B. Dame *et al.*, *Science* **225**, 593 (1984).
21. V. Enea *et al.*, *ibid.*, p. 628.
22. R. L. Coppel *et al.*, *Nature (London)* **310**, 789 (1984).
23. M. Koenen *et al.*, *ibid.* **311**, 382 (1984).
24. F. Sanger, S. Nicklen, R. Coulson, *Proc. Natl. Acad. Sci. U.S.A.* **74**, 5463 (1977).
25. J. Messing and J. Viera, *Gene* **19**, 269 (1982).
26. Yeast strain D13-1A was provided by H. Klein. We thank H. Klein for help and advice on yeast transformation, B. Hall for providing the vector, R. Gwadz for the monkey sera, S. Projan for help with the densitometer scans, and S.-C. Chiang for technical assistance. Supported by National Institute of Allergy and Infectious Diseases grant 1 R01 AI21496-01 and World Health Organization/United Nations Development Programme/World Bank Special Programme in Training in Tropical Diseases T16/181/M2/21(G).

6 December 1984; accepted 12 February 1985

Modulation of the *sis* Gene Transcript During Endothelial Cell Differentiation in Vitro

Abstract. *Endothelial cells, which line the interior walls of blood vessels, proliferate at the site of blood vessel injury. Knowledge of the factors that control the proliferation of these cells would help elucidate the role of endothelial cells in wound healing, tumor growth, and arteriosclerosis. In vitro, endothelial cells organize into viable, three-dimensional tubular structures in environments that limit cell proliferation. The process of endothelial cell organization was found to result in decreased levels of the* sis *messenger RNA transcript and increased levels of the messenger RNA transcript for fibronectin. This situation was reversed on transition from the organized structure to a proliferative monolayer. These results suggest a reciprocity for two biological response modifiers involved in the regulation of endothelial cell proliferation and differentiation in vitro.*

The abluminal surface of the vascular tree consists of a nonthrombogenic monolayer of endothelial cells that functions as a metabolic interface between blood and tissue (*1*). Damage to the vessel wall signals the endothelial cell to migrate and divide at the site of injury (*1*), events critically important for maintenance of the structural integrity of the vascular system. Indeed, neovascularization contributes significantly to controlling the growth of tumors, the maximum size of which would otherwise be limited by diffusion rate (*2*). Thus, characterization of the factors controlling endothelial cell division is important in determining the role of the endothelial cell in atherogenesis, wound healing, and tumor growth.

Human endothelial cells isolated from diverse blood vessels have been successfully propagated in vitro (*3*). The growth of human endothelial cells in vitro is controlled by endothelial cell growth factor (ECGF), a potent polypeptide mitogen isolated from bovine brain (*4*). Withdrawal of ECGF from the human endothelial cell monolayer results in a rearrangement of the cells within the monolayer into viable three-dimensional tubular structures that have a lumen and thus resemble microvessels (*5*). Although the precise polarity of the tubular structures is unknown, the relative ease with which human endothelial cells may be grown in vitro and manipulated so as to form organized structures readily lends itself to the study of the molecular biology of this phenomenon.

We used Northern blot analysis to study gene expression in proliferating and organized human endothelial cells. Because human endothelial cells produce a platelet-derived growth factor (PDGF)–like mitogen (*6*), and c-*sis* is considered to be the gene encoding for the larger of the two heterodimeric chains of PDGF (*7*), we analyzed the intracellular content of PDGF messenger RNA (mRNA) with nick-translated v-*sis* complementary DNA (cDNA) as a probe. In parallel experiments, we examined fibronectin mRNA content. Fibronectin is a structural component of the extracellular matrix and is the mediator of endothelial cell migration and attachment to collagen (*1, 5, 8*). Furthermore, fibronectin is invariably involved in the process of endothelial cell organization (*5*).

Endothelial cells from human umbilical vein were grown in fibronectin-coated plastic roller bottles in Medium 199 supplemented with fetal bovine serum and ECGF (Fig. 1A). For induction of capillary tube formation, cells from confluent monolayers were collected by treatment with trypsin and reintroduced into the original culture vessels (*5*). The cells that were exposed to the trypsin-treated human endothelial cell matrix were then incubated without ECGF in medium that was changed weekly. One week after removal of ECGF, we observed profound changes in the morphology of the cells in the newly established monolayer. At this stage the endothelial cells had begun to migrate and to organize into aligned clusters (Fig. 1B). After prolonged culture (5 weeks) in the ab-